HHS Public Access

Author manuscript

J Innate Immun. Author manuscript; available in PMC 2015 July 08.

Published in final edited form as:

J Innate Immun. 2014 ; 6(6): 860–868. doi:10.1159/000363699.

Novel role of the antimicrobial peptide LL-37 in the protection of neutrophil extracellular traps against degradation by bacterial nucleases

Ariane Neumann[a,*], **Lena Völlger**[a,*], **Evelien T.M. Berends**[b], **E. Margo Molhoek**[c], **Daphne A.C. Stapels**[d], **Marika Midon**[e], **Ana Friães**[f], **Alfred Pingoud**[e], **Suzan H.M. Rooijakkers**[b], **Richard L. Gallo**[f], **Matthias Mörgelin**[g], **Victor Nizet**[h], **Hassan Y. Naim**[a], and **Maren von Köckritz-Blickwede**[a]

[a]Department of Physiological Chemistry, University of Veterinary Medicine Hannover, 30559 Hannover, Germany [b]Medical Microbiology, University Medical Center, 3584 CX Utrecht, Netherlands [c]TNO Earth, Environmental and Life Sciences, Department CBRN protection, 2280 AA Rijswijk, The Netherlands [d]Institute of Biochemistry, Justus-Liebig University Giessen, 35392 Giessen, Germany [e]Instituto de Microbiologia, Faculdade de Medicina de Lisboa, 1649-028 Lisboa, Portugal [f]Division of Dermatology, Department of Medicine, University of California San Diego, San Diego, CA 92122 [g]Division of Infection Medicine, Department of Clinical Sciences, Biomedical Center, Lund University, Lund, Sweden [h]Department of Pediatrics and Skaggs School of Pharmacy & Pharmaceutical Sciences, University of California San Diego, La Jolla, CA 92093

Abstract

Neutrophil extracellular traps (NETs) have been described as a fundamental innate immune defense mechanism. These NETs consist of a nuclear DNA backbone associated with different antimicrobial peptides (AMPs), which are able to engulf and kill pathogens. The AMP LL-37, a member of the cathelicidin family, is highly present in NETs. However, the function of LL-37 within the NETs is still unknown, since LL-37 loses its antimicrobial activity when bound to DNA in the NETs.

Using immunofluorescence microscopy we demonstrate that NETs treated with LL-37 were distinctly more resistant to *S. aureus* nuclease degradation compared to non-treated NETs. Biochemical assays utilising a random LL-37-fragment library indicate that the blocking effect of LL-37 on nuclease activity is based on the cationic character of the AMP, which facilitates the binding to neutrophil DNA, thus protecting it from degradation by the nuclease. In good correlation to these data, the cationic AMPs human beta defensin-3 (hBD-3) and human neutrophil peptide-1 (HNP-1) showed similar protection of neutrophil-derived DNA against nuclease degradation. In conclusion, this study demonstrates a novel role of AMPs in host immune defence: Besides its direct antimicrobial activity against various pathogens, cationic AMPs can stabilise neutrophil-derived DNA or NETs against bacterial nuclease degradation.

Correspondence: Dr. Maren von Köckritz-Blickwede, Department of Physiological Chemistry, University of Veterinary Medicine Hannover, Bünteweg 17, 30559 Hannover, Germany; mkoeckbl@tiho-hannover.de; phone: +49-511-953-8787; fax: +49-511-953-8585.

*Contributed equally to the work.

Keywords

neutrophil extracellular traps (NETs); antimicrobial peptide; nuclease; cathelicidin; human neutrophil peptide-1 (HNP-1); human beta defensin 3 (hBD3)

Introduction

Classically, two strategies by which neutrophils serve as a first line of defence against invading pathogens were understood: the secretion of antimicrobial peptides (degranulation) and the engulfment of bacteria (phagocytosis) [1, 2]. More recently, Brinkmann et al. characterised neutrophil extracellular traps (NETs) as a novel additional antimicrobial function of these specialised leukocytes [3]. NET formation (NETosis) can be activated by pathogens, such as bacteria, pro-inflammatory cytokines or different substances like LPS, M protein-fibrinogen complexes, or phorbol 12-myristate 13-acetate (PMA) [4].

The backbone of NETs is nuclear DNA, as nuclease treatment results in the disruption of their structure [5]. As a mechanism of innate immune evasion, nucleases secreted by Gram-positive bacterial pathogens such as group A streptococci (GAS), *Streptococcus pneumoniae* and *Staphylococcus aureus* degrade NETs to promote neutrophil resistance and spread of infection *in vivo* [6–9].

Besides DNA, NETs are comprised of histones, several granule proteins and antimicrobial peptides (AMPs), such as the cationic pro-inflammatory peptide cathelicidin LL-37 [10–12]. Human LL-37 is a member of the cathelicidin family of mammalian cationic AMPs. LL-37 derives its name from the amino acids sequence (37 amino acids) starting with two leucine residues. It gains antimicrobial activity after maturation through cleavage of the pro-protein hCAP-18 by the serine protease proteinase 3 and adoption of the alpha-helical, amphipathic configuration of the mature peptide [13]. LL-37 is constitutively expressed in neutrophils [14], mast cells, natural killer cells (NK cells) and epithelial cells; during infections it can also be expressed by keratinocytes. During inflammatory responses, the expression of LL-37 is increased several-fold [15].

Previous studies have observed a correlation between bacterial resistance to LL-37 killing and their resistance to NET-mediated killing [16, 17]. Consequently, it was inferred that the high local concentration of LL-37 in NETs could be a critical contributor to the antimicrobial activity of the NETs [16, 17]. However, Weiner et al. showed that LL-37 can lose antimicrobial activity when bound to DNA [18]. Thus, even though LL-37 is found within NETs, its precise function in NETs remains unclear. Therefore the goal of this study was to investigate the role of LL-37 in NET formation and stability.

Methods

Isolation of neutrophils and neutrophil-derived DNA

Primary blood-derived neutrophils were isolated from fresh blood of healthy donors by density gradient centrifugation using Polymorphprep™ (Progen Biotechnik) as previously described [19]. DNA was isolated with the NucleoSpin Blood™ kit (Macherey-Nagel)

according to the manufacturer's recommendation. For *in vitro* NET assays, the cells were seeded on poly-L-lysine-coated glass slides in 24-well plates at a concentration of 5×10^5 cells/well (250μl/well) or on 48-well plates at a concentration of 2×10^5 cells/well (100μl/well). RPMI without phenol red (PAA) was used for cultivation of the cells at 37°C and 5% CO_2.

Bacterial strains and nucleases

S. aureus nuclease (micrococcal nuclease) was purchased from Cell Systems (Troisdorf). Recombinant EndA H160G (10 nM) in combination with 20 mM Tris, 5mM $MgCl_2$, 50 mM imidazole (pH 8) was used as previously described [20]. We used a panel of nuclease (*nuc*)-deficient mutants and nuclease-producing control strains of *S. aureus* USA300 LAC strain: *S. aureus* LAC wild type empty vector control (wt + pCM28), *nuc*-mutant empty vector control (*nuc* + pCM28) and complemented mutant strain *(nuc* + pCM28*nuc*) [9]. Furthermore, the following three different nuclease-producing GAS strains isolated from infected patients in Portugal were used: 2004V0695P (*emm* type 1, GAS 1), SH1131A (*emm* type 1, GAS 2), 2003V1350P (*emm* type 4, GAS 3) [21]. The bacteria were grown in Todd-Hewitt-Broth (THB, GAS) or Brain-Heart Infusion broth (BHI, *S. aureus*) to mid-log growth phase. The bacteria were then centrifuged at 3000 × *g* for 10 min, 1 ml of the supernatant was sterile-filtered with 0.4 μm filter and transferred into a new reaction tube. These supernatant samples were stored at −20°C until further usage in DNA degradation assays.

NET degradation by S. aureus nuclease

For NET-induction, neutrophils were stimulated with 25 nM PMA (in the presence or absence of 40 μg/ml aprotinin (Sigma)) and incubated for 4 h at 37°C 5% and CO_2. Next, LL-37 was added to a final concentration of 5 μM to each well followed by incubation for 30 min. Finally, 50 μl micrococcal nuclease (MN) from *S. aureus* was added to give a final concentration of 0.01 U/ml per well after which the plate was incubated for 1 h 37°C and 5% CO_2. Cells were fixed with 4% PFA and NETs were visualised as described below.

Visualisation of NETs

Fixed cells were washed three times with PBS, permeabilised and blocked with 2% BSA in 0.2% Triton X-100/PBS for 45 min at room temperature. Incubation with a mouse monoclonal anti-H2A-H2B-DNA complex (clone PL2-6) [22], 0.5 μg/ml in 2% BSA in 0.2% Triton X-100/PBS) was carried out overnight at 4°C, followed by washing (3 times with PBS) and subsequent incubation with an Alexa-Fluor-488-labelled goat-anti-mouse antibody for 45 min at room temperature. After washing, slides were mounted in ProlongGold® antifade with DAPI (Invitrogen) and analysed by confocal fluorescence microscope using a Leica TCS SP5 confocal microscope with a HCX PL APO 40× 0.75–1.25 oil immersion objective. Settings were adjusted with control preparations using an isotype control antibody. For each preparation, three randomly selected images were acquired and used for quantification of NETs. Data were expressed as area covered with NETs. The mean value derived from $n = 6$ images for each condition per experiment was used for statistical analysis.

Immunostaining of LL-37

Immunostaining of LL-37 was performed using a similar immunostaining protocol as described above for the visualisation of NETs. A polyclonal rabbit-anti-LL-37 antibody was used at a final concentration of 1.6 μg/ml [23]. Subsequently, samples were incubated with Alexa-Fluor-488 goat-anti-mouse (1:1000; Invitrogen) and an Alexa-Fluor-633 goat-anti-rabbit antibody (1:1000, Invitrogen). Again, microscope settings were adjusted with control preparations using respective isotype control antibodies.

Entrapment assay

The entrapment assay was performed as previously described [9]. Briefly, NET-producing neutrophils incubated in the presence or absence of LL-37 for 30 min (as described above) were infected with FITC-labelled *S. aureus* USA300 LAC strain for 30 min. Percentage of entrapment was calculated compared to total amount of surviving cfu under the respective conditions in the presence or absence of LL-37.

Negative staining and transmission electron microscopy

Human primary blood-derived neutrophils were isolated and treated as described above. The binding between LL-37 and DNA from neutrophil NETs was visualised by negative staining and electron microscopy as previously described [24]. LL-37 was conjugated with 5 nm colloidal gold particles according to routine protocols [25]. LL-37-Au conjugates were incubated with DNA for 30 min at RT and negatively stained with 0.75% uranyl formate. Specimens were examined in a Philips/FEI CM100 BioTwin transmission electron microscope at a ×100,000 magnification.

DNA degradation assay with DNA-intercalating dyes

The Quant-iT™ PicoGreen® dsDNA reagent and Sytox® green nucleic acid stain (Invitrogen) were used to measure degradation of host DNA. Calf thymus DNA (Sigma) or blood-derived neutrophil DNA at a final concentration of 5 μg/ml was added to a pureGrade™ black 96-well-plate (Brand). Next, LL-37 (final concentration of 5 μM) and micrococcal nuclease (final concentration of 100U/ml) or the bacterial supernatants were added. The plate was incubated for 1 h at 37°C. Then Quant-iT™ PicoGreen® dsDNA reagent or Sytox® Green nucleic acid stain was added as recommended by the manufacturer. Fluorescence was measured with the Optima FluoStar (BMG Labtech) with excitation at 485 nm and emission at 520 nm with optimized gain settings that were used throughout a similar set of experiments. HNP-1 and hBD3 (Anaspec), full length LL-37 and a fragment library of 8 different LL-37 fragments with overlapping sequences and varying biochemical properties [26] and a scrambled form of LL-37 (Anaspec) were used.

Ethidium bromide gel

A total amount of 10 μg/ml calf thymus DNA was incubated with 5 μM LL-37 for 1 h at 37°C. Ethidium bromide (Sigma) was added to give a concentration of 0.5 μg/ml. Lastly, 6× loading dye was added and 20 μl of each sample was run on a 1% agarose gel for visual examination of DNA.

Immunodotblot determination of LL-37 in NETs

Neutrophils were stimulated with 25 nM PMA for 4 h, centrifuged for 5 min at 370×g and then incubated in the presence of 0.01 U/ml MN to degrade NETs. The supernatant was harvested before (released LL-37) and after nuclease treatment (LL-37 associated with NETs) and 200 μl were spotted on a PVDF-membrane using a Dotblotting vacuum system (Carl Roth). After blocking of the membrane in 5% nonfat dry milk in PBS-Tween (0.1% Tween 20) for 45 min at constant agitation, the membrane was incubated with a 0.49 μg/ml polyclonal rabbit anti-LL-37-antibody overnight at 4°C with agitation. After washing with Tween-PBS, the membrane was incubated with the secondary goat-anti-rabbit HRP-conjugated IgG (Biorad) for 45 min at room temperature under agitation. After subsequent washing, the LL-37 signal was detected using the Super Signal®West Femto, Maximum Sensitivity Substrate (Thermo Scientific) as recommended by the manufacturer.

Statistical analysis

Data were analysed using Excel 2003 (Microsoft) and GraphPad Prism 5.0 (GraphPad Software). All experiments were performed at least three times. NET experiments were performed with blood from three different blood donors. Differences between the two groups were analysed by using a one-tailed Student's t-test. The significance is indicated as *$p<0.05$; **$p< 0.005$ and ***$p< 0.001$.

Results and discussion

LL-37 protects host DNA and NETs against degradation by bacterial nucleases

LL-37 has been shown to be associated with DNA fibres of NETs [10–12]. Immunofluorescence and electron microscopy confirmed that high amount of LL-37 is present in NETs (Figure 1A and B). Immunodotblot experiments revealed that an average of 42.5 ± 12.2% (n=4 experiments) of the LL-37 that is released by PMA-activated neutrophils, is associated with the NET fibres. LL-37 has earlier been shown to protect bacterial plasmid DNA and mammalian DNA against degradation by serum nucleases [12, 27]. Therefore, we analysed the effects of LL-37 on the stability of neutrophil DNA and/or NETs when treated with *S. aureus* nuclease. Human blood-derived neutrophils were treated with 25 nM PMA for 4 h to induce NET formation [5]. Subsequently, the induced NETs were treated with 0.01 U/ml *S. aureus* nuclease in the presence or absence of externally added LL-37. As shown in Figure 1 C and D, addition of LL-37 significantly protected NETs against degradation. When treating the cells with aprotinin to block the proteinase 3-mediated activation of endogenous, neutrophil-derived LL-37 [28], a significantly higher degree of NET degradation by *S. aureus* nuclease was detectable (Figure 1 C and D).

To study the effect of LL-37 on stabilisation of host DNA in more detail, we adopted a biochemical assay using the fluorescent dye PicoGreen to provide a precise method of monitoring nuclease activity *in vitro*. PicoGreen is a sensitive fluorescent dye widely used in analytical protocols in which double-stranded DNA (dsDNA) detection is needed [29]. The dye associates with dsDNA through intercalation, minor-groove binding, and electrostatic interactions resulting in a significant increase in fluorescence compared to the fluorescence

of the free dye in solution [30]. Small fragments of DNA (as when dsDNA is treated with nuclease) interact only weakly with PicoGreen, resulting in a decrease in fluorescence.

Correlating well with our microscopy data, addition of LL-37 significantly protected neutrophil as well as calf thymus derived DNA against degradation by *S. aureus* nuclease and resulted in a higher fluorescence signal compared to its LL-37-free control (Figure 2A and 2B). Interestingly, LL-37 alone decreased the PicoGreen signal, indicating that LL-37 binds to DNA and thereby blocks the DNA-PicoGreen interaction and subsequent fluorescence signal. This indicates that protection of DNA against nuclease degradation is the result of LL-37-mediated sequestration of the DNA. This effect is concentration-dependent: the more LL-37 that is added to the DNA, the lower is the DNA-PicoGreen signal that is detected (Figure 2D). Similar results were observed with other DNA-intercalating dyes. The presence of LL-37 decreased the ethidium bromide signal in an agarose gel based DNA detection system (Figure 2E) and DNA detection with the fluorescent dye Sytox green using a fluorimeter (Figure 2C). Thus, LL-37 interferes with DNA-intercalating dyes and therefore this might not be the method of choice to visualise NETs. As shown in Figure 3, a DNA intercalating dye as DAPI is not efficient enough to visualise the complete structure of a NET. In contrast, an antibody-mediated method e.g. an antibody against histone-DNA-complexes as used here, is giving a more complete image of the NETs structure.

Despite interference of LL-37 with the PicoGreen signal, the assay is still sensitive enough for determining the degradation of DNA by bacterial nucleases and its protection by LL-37 (Figure 2 A–C). Next, we determined if LL-37 is also able to protect the DNA against degradation by nucleases derived from other bacterial species. Similar to *S. aureus* nuclease, LL-37 was also able to protect the DNA against degradation by purified EndA from *S. pneumoniae* (Figure 4A) and by nucleases from three different nuclease-producing GAS strains (Figure 4B). Furthermore, LL-37 was able to protect the DNA against degradation mediated by the prototype community-acquired methicillin-resistant *S. aureus* (MRSA) strain USA300 LAC (Figure 4C). In this experiment the supernatant of an isogenic nuclease mutant strain (*nuc*) was used as a negative control. In the absence of LL-37, the supernatant of nuclease-producing WT MRSA strain showed significant higher DNA degradation compared to the supernatant of nuclease-deficient strain. In the presence of LL-37, the nuclease activity was blocked and all supernatants yielded similar DNA levels (Figure 4C).

Taken together, we here demonstrate a novel role of the AMP LL-37, the protection of neutrophil DNA and NETs against degradation by bacterial nucleases. Accordingly, an electron micrograph of NETs after degradation with purified and highly concentrated micrococcal nuclease revealed shortened left-over NET-structures that are decorated with gold-labelled LL-37 (Figure 4D). All parts of the NETs that have not been decorated with LL-37 (as partially seen in Figure 1B) have been enzymatically degraded and are not visible anymore. Importantly, a functional assay analysing the entrapment of MRSA USA300 LAC in the presence or absence of LL-37 revealed a distinct ($p=0.05$) increase of entrapment of surviving cfu in the presence of 5 μM LL-37. Thus, LL-37 might not only efficiently kill bacteria [31] or increase antimicrobial activities of neutrophils [32] as previously shown, but also enhances NET-mediated entrapment and subsequent immobilization of bacteria.

The positive overall charge of LL-37 is responsible for LL-37-mediated stabilisation of host DNA against bacterial nucleases

With our next experiments we aimed to determine biochemical features causing LL-37-mediated protection of host DNA against bacterial nuclease degradation. The PicoGreen assay was conducted using the fragment library of LL-37 fragments with overlapping sequences (Figure 5A) and a scrambled form of the peptide with the same amino acid composition serving as a control. As shown in Figure 5B, in addition to the full-length LL-37 peptide, fragments LL-31 and RK-25 were able to stabilise the DNA. A statistical analysis using the Pearson correlation test confirmed that the cationicity correlates with the ability to protect the DNA against nuclease degradation.

To verify that cationicity is involved in the phenomenon of DNA stabilisation, two other well-characterised human cationic AMPs, HNP-1 and hBD-3, were tested in an identical assay. In Figure 5C and D it is shown that both peptides significantly diminish DNA degradation by *S. aureus* nuclease; however, neither peptide protects the DNA against nuclease degradation to the degree that LL-37 affords protection (Figure 5C and D). These data imply that a cocktail of different host-derived cationic peptides may function in concert to stabilise NETs against bacterial nucleases.

Conclusions

Here we show that LL-37 protected NETs, purified neutrophil DNA, and calf thymus DNA against degradation mediated by nucleases derived from bacterial pathogens including *S. aureus*, *S. pneumoniae* and GAS. Nuclease production by these pathogens can protect against NET-mediated entrapment and immobilisation in case of *S. pneumoniae* as well as NET-mediated bacterial killing in case of GAS and *S. aureus* [6–9]. However, residual NETs can still be detected in the tissue of mice infected with nuclease-producing bacteria as shown for *S. aureus* [9], indicating an incomplete degradation by bacterial nucleases *in vivo* based on a stabilisation by host factors.

Thus, the abundance of the cathelicidin AMP within NETs may not be an accidental by-product of simultaneous NETosis and degranulation, but may reflect an integral role of the peptide in NET formation and longevity.

Acknowledgments

We wish to thank Marc Monestier, Temple University School of Medicine, Philadelphia, PA, for kindly providing us the H2A-H2B-DNA complex antibody and Mário Ramirez, Faculty of Medicine, University of Lisbon, Portugal, for providing the GAS strains.

Funding

This work was supported in part by DFG grant KO 3552/4-1, NIH grants AI052453 and AR052728 (RG, VN) and a Vidi grant from the Dutch Scientific Organisation NWO (S.H.M.R., E.T.M.B., D.A.C.S.).

References

1. Lehrer RI, Ganz T. Antimicrobial peptides in mammalian and insect host defence. Curr Opin Immunol. 1999; 11:23–27. [PubMed: 10047545]

2. Tauber A. The birth of immunology. III. The fate of the phagocytosis theory. Cell Immunol. 1992; 139(2):505–530. [PubMed: 1733516]

3. Brinkmann V, Reichard U, Goosmann C, Fauler B, Uhlemann Y, Weiss DS, Weinrauch Y, Zychlinsky A. Neutrophil extracellular traps kill bacteria. Science. 2004; 303:1532–1535. [PubMed: 15001782]

4. von Köckritz-Blickwede M, Nizet V. Innate immunity turned inside-out: antimicrobial defense by phagocyte extracellular traps. J Mol Med. 2009; 87(8):775–783. [PubMed: 19444424]

5. Fuchs TA, Abed U, Goosmann C, Hurwitz R, Schulze I, Wahn V, Weinrauch Y, Brinkmann V, Zychlinsky A. Novel cell death program leads to neutrophil extracellular traps. J Cell Biol. 2007; 176(2):231–241. [PubMed: 17210947]

6. Sumby P, Barbian KD, Gardner DJ, Whitney AR, Welty DM, Long RD, Bailey JR, Parnell MJ, Hoe NP, Adams GG, Deleo FR, Musser JM. Extracellular deoxyribonuclease made by group A Streptococcus assists pathogenesis by enhancing evasion of the innate immune response. Proc Natl Acad Sci USA. 2005; 102(5):1679–1684. [PubMed: 15668390]

7. Beiter K, Wartha F, Albiger B, Normark S, Zychlinsky A, Henriques-Normark B. An endonuclease allows *Streptococcus pneumoniae* to escape from neutrophil extracellular traps. Curr Biol. 2006; 16:401–407. [PubMed: 16488875]

8. Buchanan JT, Simpson AJ, Aziz RK, Liu GY, Kristian SA, Kotb M, Feramisco J, Nizet V. DNase expression allows the pathogen group A streptococcus to escape killing in neutrophil extracellular traps. Curr Biol. 2006; 16:396–400. [PubMed: 16488874]

9. Berends ET, Horswill AR, Haste NM, Monestier M, Nizet V, von Köckritz-Blickwede M. Nuclease expression by *Staphylococcus aureus* facilitates escape from neutrophil extracellular traps. J Innate Immun. 2010; 2(6):576–586. [PubMed: 20829609]

10. Chow OA, von Köckritz-Blickwede M, Bright AT, Hensler ME, Zinkernagel AS, Cogen AL, Gallo RL, Monestier M, Wang Y, Glass CK, Nizet V. Statins enhance formation of phagocyte extracellular traps. Cell Host Microbe. 2010; 8(5):445–454. [PubMed: 21075355]

11. Urban CF, Ermert D, Schmid M, Abu-Abed U, Goosmann C, Nacken W, Brinkmann V, Jungblut PR, Zychlinsky A. Neutrophil extracellular traps contain calprotectin, a cytosolic protein complex involved in host defense against Candida albicans. PLoS Pathog. 2009; 5(10):e1000639. [PubMed: 19876394]

12. Lande R, Ganguly D, Facchinetti V, Frasca L, Conrad C, Gregorio J, Meller S, Chamilos G, Sebasigari R, Riccieri V, Bassett R, Amuro H, Fukuhara S, Ito T, Liu YJ, Gilliet M. Neutrophils activate plasmacytoid dendritic cells by releasing self-DNA-peptide complexes in systemic lupus erythematosus. Sci Transl Med. 2011; 3(73):73ra19.

13. Sörensen OE, Follin P, Johnsen AH, Calafat J, Tjabringa GS, Hiemstra PS, Borregaard N. Human cathelicidin, hCAP-18, is processed to the antimicrobial petide LL-37 by extracellular cleavage with proteinase 3. Blood. 2001; 97(12):3951–3959. [PubMed: 11389039]

14. Zanetti M, Gennaro R, Romeo D. Cathelicidins: a novel protein family with a common proregion and a variable C-terminal antimicrobial domain. FEBS Let. 1995; 374(1):1–5. [PubMed: 7589491]

15. Lai Y, Gallo RL. AMPed up immunity: how antimicrobial peptides have multiple roles in immune defense. Trends Immunol. 2009; 30(3):131–14. [PubMed: 19217824]

16. Cole JN, Pence MA, von Köckritz-Blickwede M, Hollands A, Gallo RL, Walker MJ, Nizet V. M protein and hyaluronic acid capsule are essential for in vivo selection of covRS mutations characteristic of invasive serotype M1T1 group A Streptococcus. MBio. 2010; 1(4):e00191–10. [PubMed: 20827373]

17. Lauth X, von Köckritz-Blickwede M, McNamara CW, Myskowski S, Zinkernagel AS, Beall B, Ghosh P, Gallo RL, Nizet V. M1 protein allows group A streptococcal survival in phagocyte extracellular traps through cathelicidin inhibition. J Innate Immun. 2009; 1(3):202–214. [PubMed: 20375578]

18. Weiner DJ, Bucki R, Janmey PA. The antimicrobial activity of the cathelicidin LL37 is inhibited by F-actin bundles and restored by gelsolin. Am J Respir Cell Mol Biol. 2003; 28(6):738–745. [PubMed: 12600826]

19. von Köckritz-Blickwede, M.; Chow, O.; Ghochani, M.; Nizet, V. Visualization and functional evaluation of phagocyte extracellular traps. In: Kaufmann, S.; Kabelitz, D., editors. Immunology

of Infection. 3. Maryland Geights, MO: Acedemic Press, Elsevier Science; 2010. Series: Methods in Microbiology

20. Midon M, Schäfer P, Pingoud A, Ghosh M, Moon AF, Cuneo MJ, London RE, Meiss G. Mutational and biochemical analysis of the DNA-entry nuclease EndA from *Streptococcus pneumoniae*. Nucleic Acids Res. 2011; 39(2):623–634. [PubMed: 20846957]
21. Friães A, Ramirez M, Melo-Cristino J, Portuguese Group for the Study of Streptococcal Infections. Nonoutbreak surveillance of group A streptococci causing invasive disease in Portugal identified internationally disseminated clones among members of a genetically heterogeneous population. J Clin Microbiol. 2007; 45(6):2044–2047. [PubMed: 17460058]
22. Losman MJ, Fasy TM, Novick KE, Monestier M. Monoclonal autoantibodies to subnucleosomes from a MRL/Mp (−)+/+ mouse. Oligoclonality of the antibody response and recognition of a determinant composed of histones H2A, H2B, and DNA. J Immunol. 1992; 148(5):1561–1569. [PubMed: 1371530]
23. Dorschner RA, Pestonjamasp VK, Tamakuwala S, Ohtake T, Rudisill J, Nizet V, Agerberth B, Gudmundsson GH, Gallo RL. Cutaneous injury induces the release of cathelicidin anti-microbial peptides active against group A Streptococcus. J Invest Dermatol. 2001; 117(1):91–97. [PubMed: 11442754]
24. Bober M, Enochsson C, Collin M, Mörgelin M. Collagen VI is a subepithelial adhesive target for human respiratory tract pathogens. J Innate Immun. 2010; 2:160–166. [PubMed: 20375633]
25. Baschong W, Wrigley NG. Small colloidal gold conjugated to Fab fragments or to immunoglobulin G as high-resolution labels for electron microscopy: a technical overview. J Electron Microsc Tech. 1990; 14:313–323. [PubMed: 2332806]
26. Molhoek EM, den Hertog AL, de Vries AM, Nazmi K, Veerman EC, Hartgers FC, Yazdanbakhsh M, Bikker FJ, van der Kleij D. Structure-function relationship of the human antimicrobial peptide LL-37 and LL-37 fragments in the modulation of TLR responses. Biol Chem. 2009; 390(4):295–303. [PubMed: 19166322]
27. Sandgren S, Wittrup A, Cheng F, Jönsson M, Eklund E, Busch S, Belting M. The human antimicrobial peptide LL-37 transfers extracellular DNA plasmid to the nuclear compartment of mammalian cells via lipid rafts and proteoglycan-dependent endocytosis. J Biol Chem. 2004; 279(17):17951–17956. [PubMed: 14963039]
28. Yamasaki K, Schauber J, Coda A, Lin H, Dorschner RA, Schechter NM, Bonnart C, Descargues P, Hovnanian A, Gallo RL. Kallikrein-mediated proteolysis regulates the antimicrobial effects of cathelicidins in skin. FASEB J. 2006; 20(12):2068–2080. [PubMed: 17012259]
29. Singer VL, Jones LJ, Yue ST, Haugland RP. Characterization of PicoGreen reagent and development of a fluorescence-based solution assay for double-stranded DNA quantitation. Anal Biochem. 1997; 249:228–238. [PubMed: 9212875]
30. Dragan AI, Casas-Finet JR, Bishop ES, Strouse RJ, Schenerman MA, Geddes CD. Characterization of PicoGreen interaction with dsDNA and the origin of its fluorescence enhancement upon binding. Biophys J. 2010; 99:3010–3019. [PubMed: 21044599]
31. Turner J, Cho Y, Dinh NN, Waring AJ, Lehrer RI. Activities of LL-37, a cathelin-associated antimicrobial peptide of human neutrophils. Antimicrob Agents Chemother. 1998; 42(9):2206–2214. [PubMed: 9736536]
32. Alalwani SM, Sierigk J, Herr C, Pinkenburg O, Gallo R, Vogelmeier C, Bals R. The antimicrobial peptide LL-37 modulates the inflammatory and host defense response of human neutrophils. Eur J Immunol. 2010; 40(4):1118–1126. [PubMed: 20140902]

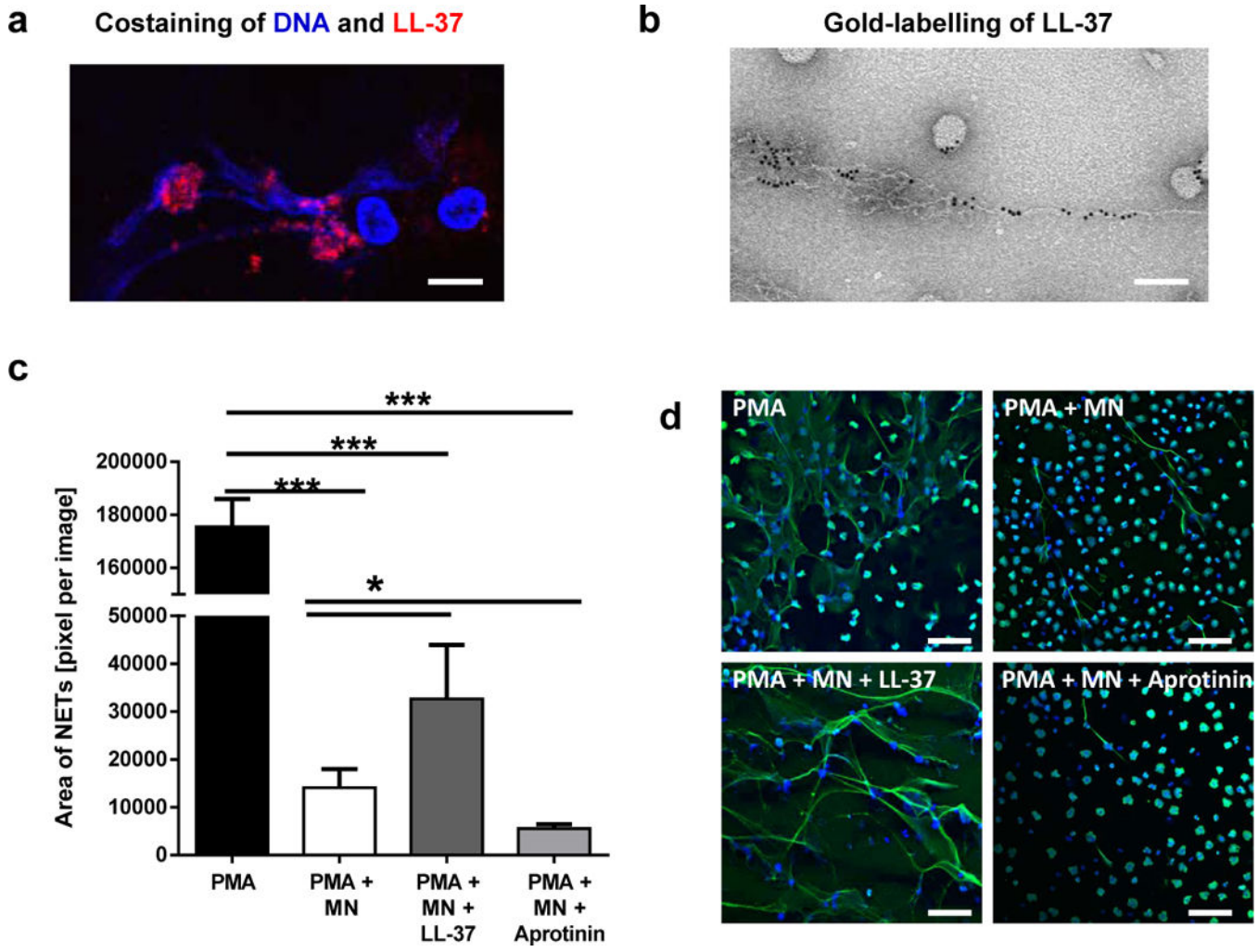

Fig. 1.

LL-37 protects NETs against degradation by *S. aureus* nuclease. (a and b) Confocal immunofluorescence (a) and electron micrograph (b) of structures e.g. NETs and nanoparticles released by PMA-activated neutrophils which are associated with a high amount of LL-37. Bar 8 μm (a) and 100 nm (b). (c) Human blood-derived neutrophils were stimulated with 25nM PMA for 4 hours to induce 100% NET formation. Aprotinin (40 μg/ml) was used to block formation of endogenous active LL-37. Then, the NETs were treated with 0.01 U/ml *S. aureus* nuclease (micrococcal nuclease, MN) in the presence or absence of externally added LL-37 (5 μM). (d) Representative fluorescent micrographs displaying the results of the column bar graph in (c). The bars indicate 50 μm. NETs were visualised using an Alexa 488-labelled antibody against H2A-H2B-DNA complexes (green) in combination with DAPI to stain the nuclei in blue. The area covered with NETs was quantified using Image J. The graph represents the mean ± SEM of minimum 18 images derived from 3 independent experiments. * $p < 0.05$, *** $p < 0.001$ by t-test.

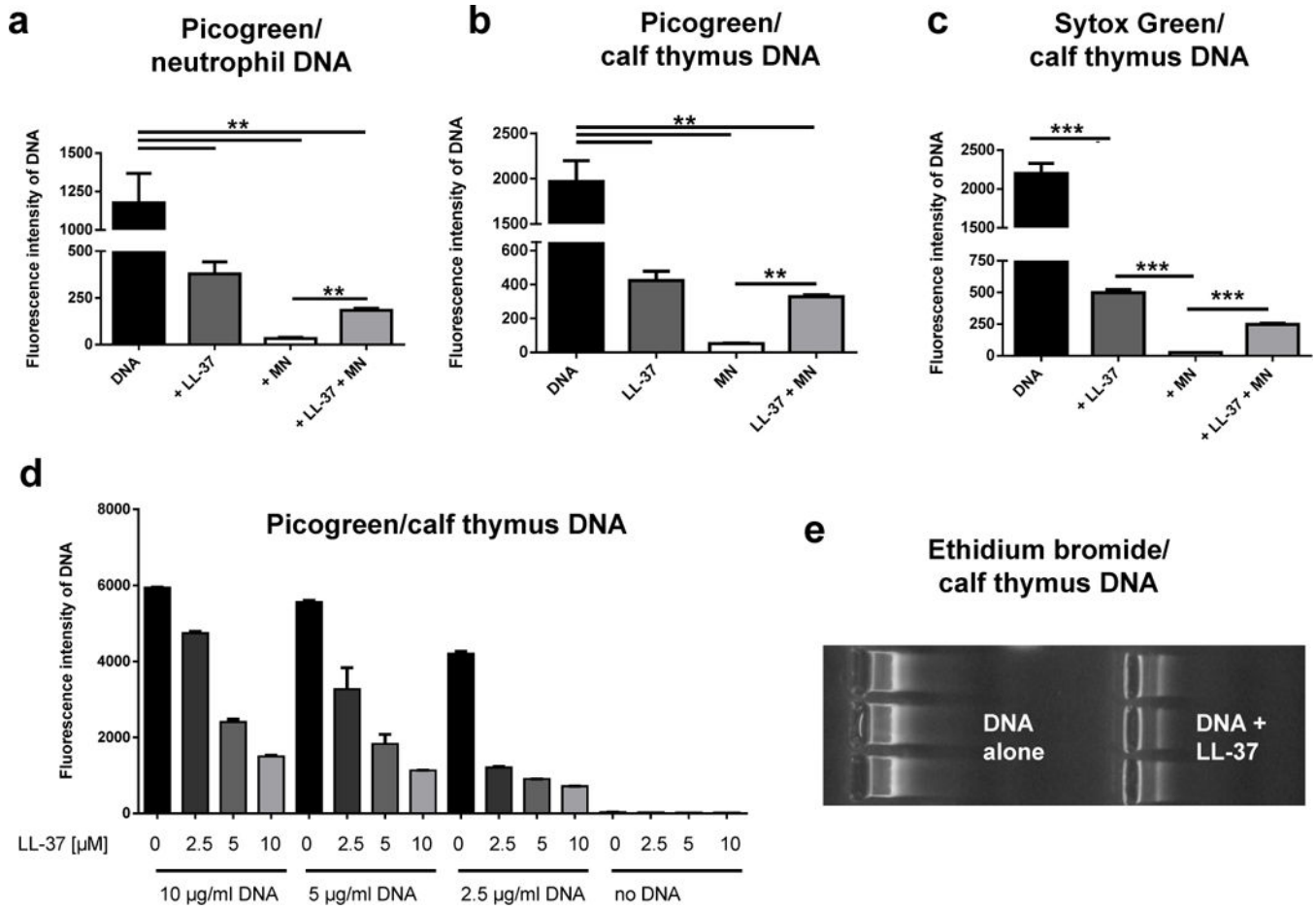

Fig. 2.

LL-37 protects host DNA against degradation by *S. aureus* nuclease. Quantification of DNA and its degradation using different DNA-intercalating dyes (PicoGreen in (a), (b) and (d); Sytox green in (c); ethidium bromide in (e)) in the presence or absence of 5 μM LL-37 ± 100 U/ml *S. aureus* nuclease (micrococcal nuclease, MN). All graphs represent the mean ± SEM of minimum 3 independent experiments. * $p < 0.05$, ** $p < 0.005$, *** $p < 0.001$ by t-test.

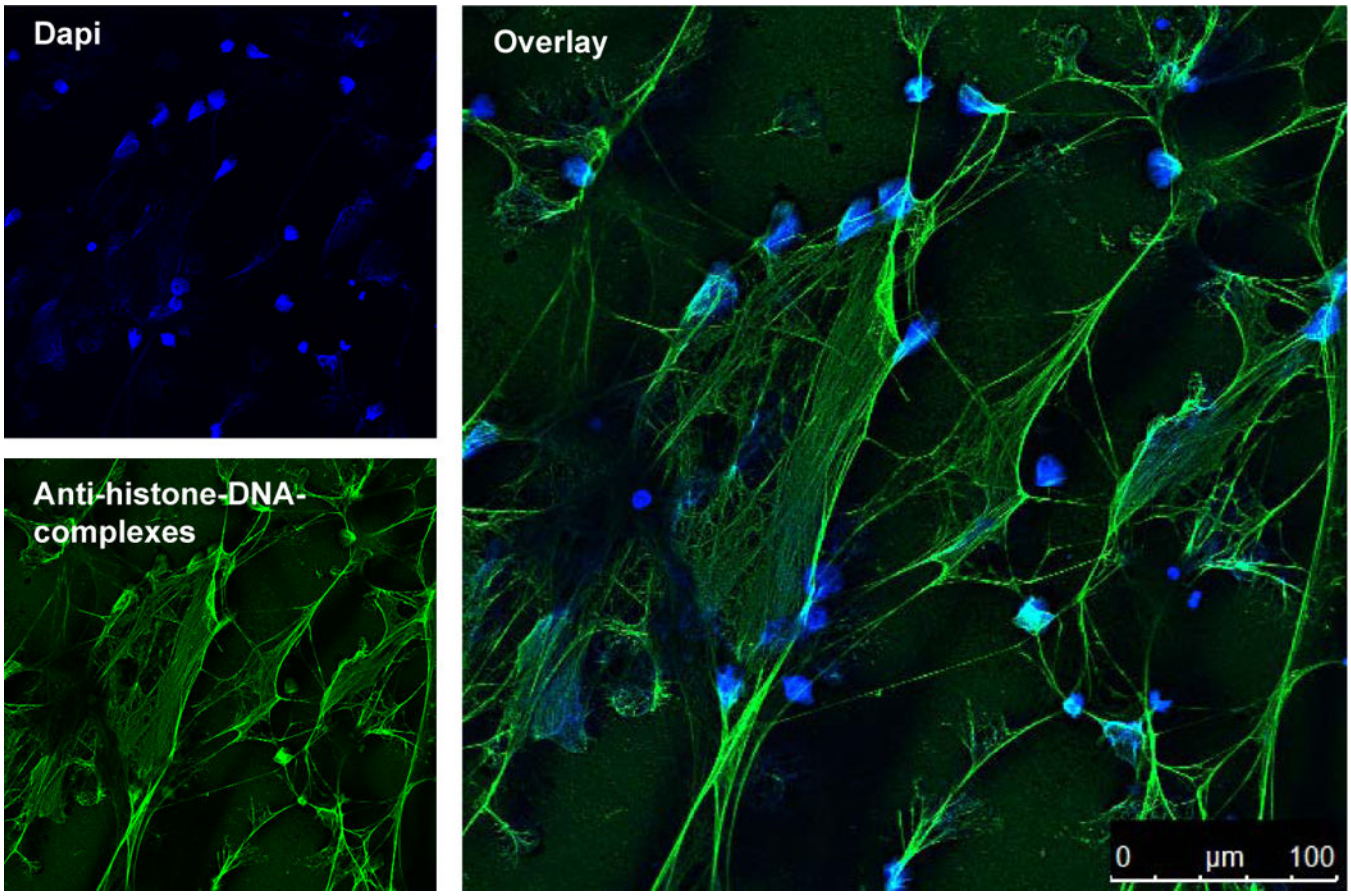

Fig. 3.

DAPI and immunostaining of NETs. Confocal immunofluorescent micrograph of NETs. NETs were visualised using an Alexa 488-labelled antibody against H2A-H2B-DNA complexes (green) and with DAPI to stain the extra- and intracellular DNA in blue.

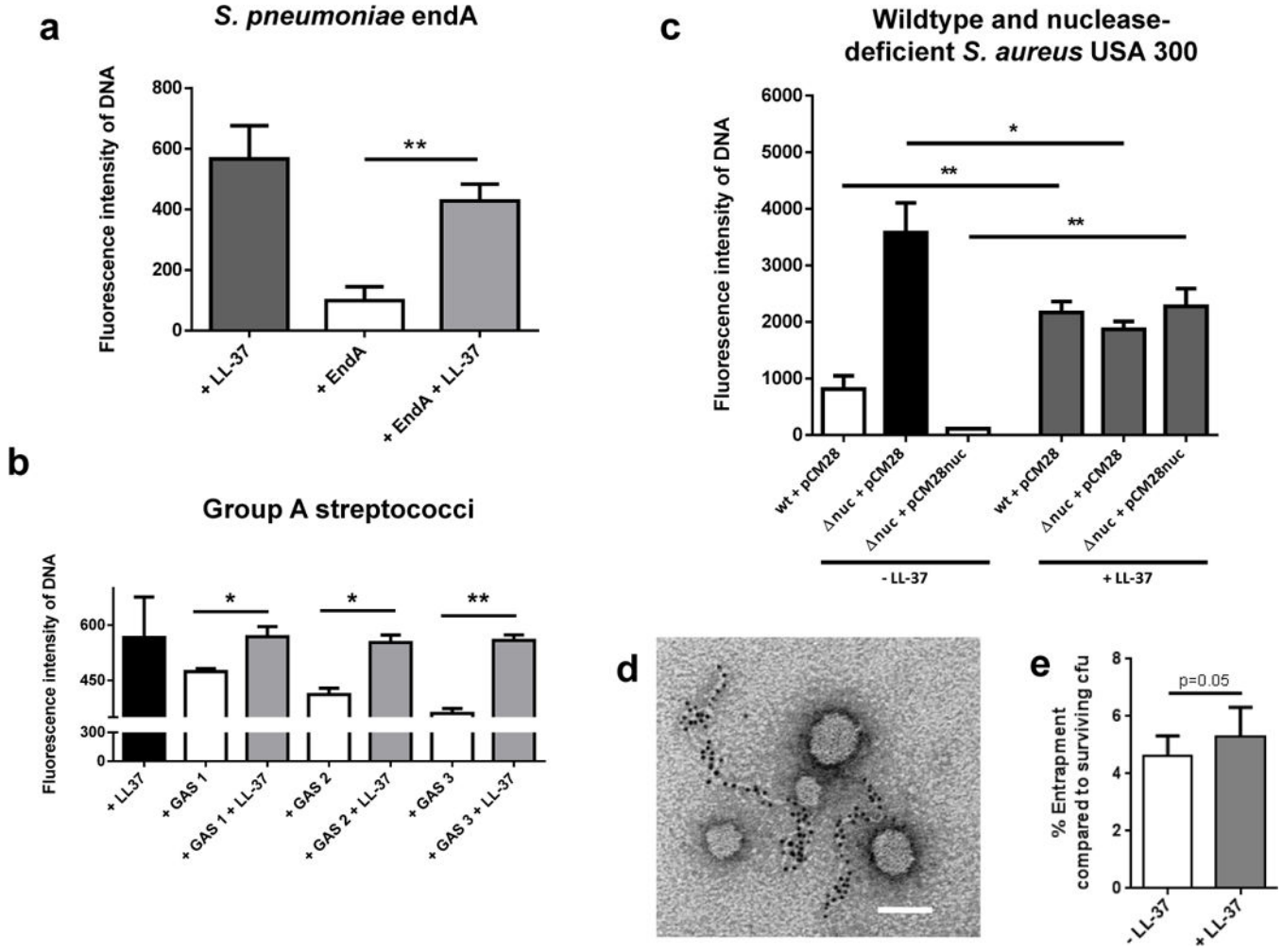

Fig. 4.

LL-37 protects host DNA against degradation by nucleases derived from different Gram-positive bacteria: DNA-degradation in the presence or absence of 5 μM LL-37 by purified EndA (a), supernatants of three different group A streptococcal (GAS) strains (b) and *S. aureus* USA300 LAC (c) using PicoGreen as a marker. In (c), a panel of nuclease (*nuc*)-deficient mutants and nuclease-producing control strains of *S. aureus* USA300 LAC strain was used: *S. aureus* LAC wild type empty vector control (wt + pCM28), *nuc*-mutant empty vector control (*nuc* + pCM28) or complemented mutant strain *(nuc* + pCM28*nuc*). Electron micrograph of NETs after degradation with purified micrococcal nuclease: Only small left-over NET-structures that are decorated with gold-labelled LL-37 are visible. All NETs that are not decorated with LL-37 (as partially seen in Figure 1b) have been enzymatically degraded and are not detectable anymore. Bar 100 nm. (d) Entrapment of *S. aureus* USA300 LAC strain by NET-releasing neutrophils in the presence of absence of 5 μM LL-37: Percentage of entrapment was calculated compared to total amount of surviving cfu under the respective conditions in the presence or absence of LL-37 (e). All graphs represent the mean ± SEM of minimum 3 independent experiments. * $p < 0.05$, ** $p < 0.005$ by t-test.

a

Peptide	Sequence	Charge	% α-helicity	Cationicity	Hydrophobicity
LL-37	***LLGDFFRKSK EKIGKEFKRI VQRIKDFLRN LVPRTES***	6	68.6	***100***	100.0
LL-31	***LLGDFFRKSK EKIGKEFKRI VQRIKDFLRN L***	6	60.9	***86.4***	101.3
LL-25	LLGDFFRKSK EKIGKEFKRI VQRIK	6	65.8	63.1	69.1
LL-19	LLGDFFRKSK EKIGKEFKR	4	39.8	50.2	59.6
IG-25	IGKEFKRI VQRIKDFLRN LVPRTES	4	41.0	65.4	89.6
IG-19	IGKEFKRI VQRIKDFLRN L	4	32.7	60.7	92.5
RK-25	***RKSK EKIGKEFKRI VQRIKDFLRN L***	7	53.7	***78.9***	85.1
RK-19	RKSK EKIGKEFKRI VQRIK	7	25.5	67.8	52.6
hBD-3	GIINTLQKYYCRVRGGRCAVLSCLPKEEQIGKCSTRGRKCCRRKK	11	unknown	unknown	unknown
HNP-1	ACYCRIPACIAGERRYGTCIYQGRLWAFCC	3	unknown	unknown	unknown
Scr. LL-37	GLKLRFEFSKIKGEFLKTPEVRFRDIKLKDNRISVQR	6	unknown	unknown	unknown

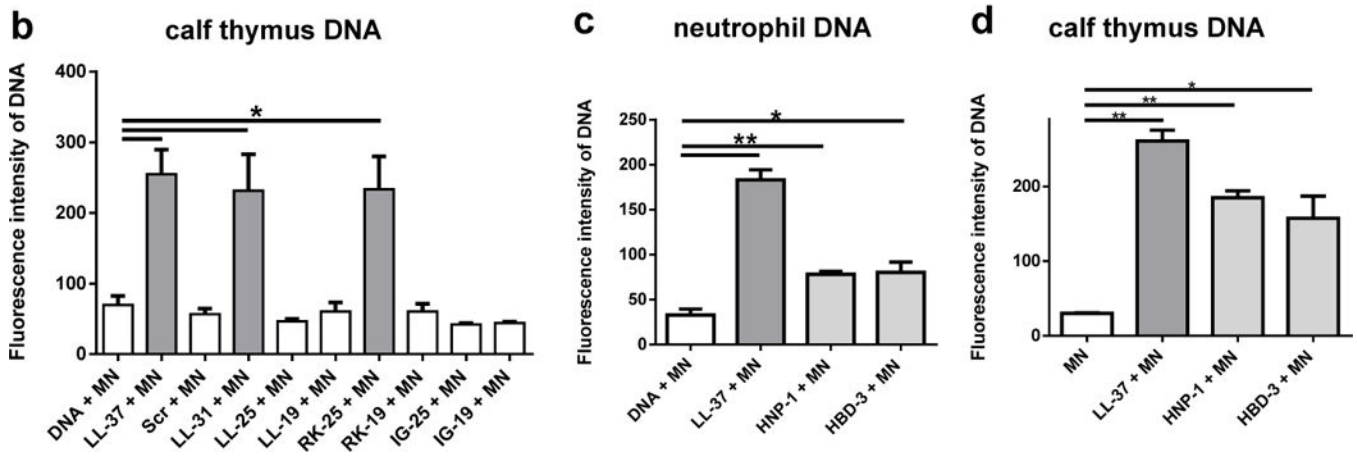

Fig. 5.

Cationicity is involved in protection of host DNA against bacterial nuclease-mediated degradation. Sequences and biochemical characteristics of LL-37, LL-37 fragments, scrambled LL-37 (Scr. LL-37), hBD-3 and HNP-1 (a). Quantification of DNA-degradation by 100 U/ml *S. aureus* nuclease (micrococcal nuclease, MN) in the presence or absence of 5 μM LL-37, LL-37 fragments, scrambled LL-37 (b) or 5 μM HNP-1 and hBD-3 ((c) and (d)). All graphs represent the mean ± SEM of minimum 3 independent experiments. * $p < 0.05$, ** $p < 0.005$ by t-test.